

- (10) L. F. Dahl, C. Martell, and D. L. Wampler, *J. Am. Chem. Soc.*, **83**, 1761 (1961).
- (11) K. R. Mann, N. S. Lewis, R. M. Williams, H. B. Gray, and J. G. Gordon II, *Inorg. Chem.*, **17**, 828 (1978).
- (12) J. A. McCleverty and G. W. Wilkinson, *Inorg. Synth.*, **8**, 211 (1966).
- (13) S. G. McGeichin, *Can. J. Chem.*, **46**, 1903 (1968).
- (14) W. R. Busing and H. A. Levy, *Acta Crystallogr.*, **22**, 457 (1967).
- (15) Computations were performed by a CDC CYBER 73 computer with the aid of the following programs: Zalkin's FORDAP Fourier program, Busing and Levy's ORFFE function and error program, and Ibers' NUCLS least-squares program. Plots of the structures were drawn with the aid of C. K. Johnson's ORTEP.
- (16) Heavy-atom scattering factors were taken from D. T. Cromer and J. B. Mann, *Acta Crystallogr., Sect. A*, **24**, 321 (1968). Hydrogen atom scattering factors were taken from "International Tables for X-Ray Crystallography", Vol. III, Kynoch Press, Birmingham, England, 1962. Anomalous scattering corrections were applied to the rhodium and fluorine atoms and were taken from D. T. Cromer, *Acta Crystallogr.*, **18**, 17 (1965).
- (17) The discrepancy indices are given by $R_1 = \sum |F_o| - |F_c| / \sum |F_o|$ and $R_2 = [(\sum w|F_o| - |F_c|)^2 / \sum w|F_o|^2]^{1/2}$.
- (18) G. W. Roberts, S. C. Cummings, and J. A. Cunningham, *Inorg. Chem.*, **15**, 2503 (1976).
- (19) K. R. Mann, J. G. Gordon II, and H. B. Gray, *J. Am. Chem. Soc.*, **97**, 3553 (1975).

Contribution from the Departments of Chemistry, Washington State University, Pullman, Washington 99164, and California Institute of Technology, Pasadena, California 91125

Molecular Structure and Magnetic Properties of the Chloro-Bridged Dimer Chloro[hydrotris(1-pyrazolyl)borato]copper(II). Observation of a Ferromagnetic Ground State

STEPHANIE G. N. ROUNDHILL,^{1a} D. MAX ROUNDHILL,*^{1a} DARREL R. BLOOMQUIST,^{1a} CHRISTOPHER LANDEE,^{1a} ROGER D. WILLETT,^{1a} DAVID M. DOOLEY,^{1b} and HARRY B. GRAY^{1b}

Received August 4, 1978

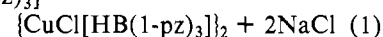
The complexes $\{\text{CuCl}[\text{HB}(1\text{-pz})_3]\}_2$ and $\text{CoCl}[\text{HB}(1\text{-pz})_3]$ have been prepared. The crystal structure of the copper(II) compound has been solved and the magnetic susceptibility measured. The compound belongs to the $P2_1/n$ space group with $Z = 2$, $a = 13.1440$ (15) Å, $b = 13.247$ (3) Å, $c = 7.467$ (13) Å, and $\beta = 96.073$ (14)°. The centrosymmetric structure has symmetric chloro bridges between the coppers leading to a distorted five-coordinate geometry about these metal centers. The geometry about each copper approximates that of a distorted square pyramid. The bridging chlorides and two ligand nitrogen atoms form the base of the pyramid, and the third ligand nitrogen occupies the axial site. The planar Cu_2Cl_2 bridge has Cu-Cl distances of 2.306 (2) and 2.316 (2) Å and a Cu-Cl-Cu angle of 94.51 (7)°. The electronic and EPR spectra are compatible with such a structure. The susceptibility data down to a temperature of 2 K show the presence of a ferromagnetically coupled ground state ($2J/k = 48.6^\circ$) for the dimer. The data have been fitted in accord with a model of Heisenberg dimers with Ising-like coupling to adjacent dimers. The complex $\text{CoCl}[\text{HB}(1\text{-pz})_3]$ shows an electronic spectrum in solution suggestive of a pseudotetrahedral geometry about Co(II).

Salts of the hydrotris(1-pyrazolyl)borate anion have been prepared by Trofimenko.² The anion is a very useful anionic tridentate chelating ligand which forms complexes with first-row transition-metal ions. The ligand is particularly amenable for coordination in the three facial positions of an octahedral complex, and a series of such complexes, $\text{M}[\text{HB}(1\text{-pz})_3]_2$, has been prepared.³ Less effort has been devoted to using the ligand for imposing a distorted four- or five-coordinate geometry about these metal ions, but this chelate ligand can potentially be used to create such a geometric environment about the metal ion. We now report our structural, spectroscopic, and magnetic results obtained with the compound $\{\text{CuCl}[\text{HB}(1\text{-pz})_3]\}_2$.

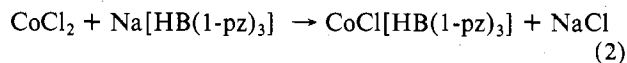
Previous structural work on hydrotris(1-pyrazolyl)borato complexes of copper has centered mainly on the copper(I) compounds. The compound $\{\text{Cu}[\text{HB}(1\text{-pz})_3]\}_2$ is bridged by the third pyrazolyl nitrogen from each hydrotris(1-pyrazolyl)borato ligand, and the geometry about the central copper(I) ion can be roughly described as a distorted tetrahedron.⁴ A crystal structure study of the carbonyl complex $\text{Cu}(\text{CO})[\text{HB}(1\text{-pz})_3]$ shows the compound to be monomeric with molecules having both precise and distorted C_{3v} symmetries about copper(I) in the unit cell.⁵ More recently the structure of the copper(I) complex $\text{K}[\text{Cu}(p\text{-NO}_2\text{C}_6\text{H}_4\text{S})[\text{HB}(3,5\text{-Me}_2(1\text{-pz})_3)]_2 \cdot (\text{CH}_3)_2\text{CO}$ has been reported, and this too has a distorted tetrahedral geometry about the metal center.⁶ It should be possible, therefore, to prepare hydrotris(1-pyrazolyl)borato complexes of divalent copper with a single monodentate ligand such as halide coordinated to the metal,

thereby placing the metal ion in an unsymmetrical environment.

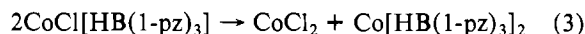
Treating anhydrous cupric chloride with an equimolar quantity of sodium hydrotris(1-pyrazolyl)borate in an ethanol or acetonitrile solvent system leads to the isolation in good yield of a copper(II) complex having the stoichiometry $\text{CuCl}[\text{HB}(1\text{-pz})_3]$ (eq 1). The complex is not monomeric but is $2\text{CuCl}_2 + 2\text{Na}[\text{HB}(1\text{-pz})_3] \rightarrow$



symmetrically bridged by chloro ligands between the copper ions. This geometric arrangement has been confirmed by a single-crystal X-ray structural study, and the electronic and EPR spectral data are in agreement with such a structure. Using a similar procedure it is possible to isolate the stoichiometrically analogous cobalt(II) complex $\text{CoCl}[\text{HB}(1\text{-pz})_3]$ (eq 2). This latter compound is very unstable to ligand



disproportionation in solution, probably because of the coordination of the strong ligand field hydrotris(1-pyrazolyl)borato chelate about a pseudotetrahedral metal ion (eq 3).



Experimental Section

Anhydrous cupric chloride was prepared by heating the hydrate at 100 °C for 12 h. Sodium hydrotris(1-pyrazolyl)borate was prepared by a published procedure. Electronic spectra were measured as

Table I. Positional and Thermal Parameters for the Nonhydrogen Atoms in $\{\text{CuCl}[\text{HB}(\text{1-pz})_3]_2\}$

atom	<i>x</i>	<i>y</i>	<i>z</i>	$\beta_{1,1}$	$\beta_{2,2}$	$\beta_{3,3}$	$\beta_{1,2}$	$\beta_{1,3}$	$\beta_{2,3}$
Cu	0.1006 (1)	0.5213 (1)	0.6573 (1)	0.0035 (1)	0.0035 (1)	0.0171 (2)	-0.0001 (1)	-0.0006 (1)	-0.0012 (1)
Cl	0.0142 (1)	0.3834 (1)	0.5290 (3)	0.0056 (1)	0.0037 (1)	0.0324 (6)	0.0003 (1)	-0.0060 (2)	-0.0018 (2)
B	0.3176 (6)	0.5685 (6)	0.8332 (10)	0.0044 (5)	0.0054 (5)	0.0110 (15)	-0.0002 (4)	-0.0006 (7)	-0.0002 (7)
N1	0.1393 (4)	0.6409 (4)	0.8113 (7)	0.0036 (3)	0.0040 (3)	0.0156 (12)	-0.0000 (3)	-0.0000 (5)	-0.0018 (5)
N3	0.2371 (4)	0.5433 (4)	0.5148 (7)	0.0046 (3)	0.0043 (4)	0.0110 (11)	0.0005 (3)	-0.0006 (5)	-0.0009 (5)
N5	0.1824 (4)	0.4358 (4)	0.8374 (7)	0.0054 (4)	0.0039 (3)	0.0153 (12)	-0.0006 (3)	0.0004 (5)	-0.0001 (5)
N2	0.2390 (4)	0.6501 (4)	0.8780 (7)	0.0041 (3)	0.0034 (3)	0.0142 (11)	-0.0007 (3)	0.0009 (5)	-0.0007 (5)
C1	0.2523 (6)	0.7355 (5)	0.9728 (9)	0.0062 (5)	0.0046 (5)	0.0144 (15)	-0.0014 (4)	0.0015 (7)	-0.0006 (7)
C2	0.1593 (6)	0.7848 (5)	0.9673 (11)	0.0070 (6)	0.0045 (5)	0.0235 (20)	-0.0008 (4)	0.0026 (8)	-0.0045 (8)
C3	0.0919 (5)	0.7216 (5)	0.8653 (10)	0.0051 (5)	0.0046 (4)	0.0206 (17)	0.0004 (4)	0.0029 (7)	-0.0017 (7)
N4	0.3227 (4)	0.5674 (4)	0.6279 (7)	0.0037 (3)	0.0037 (3)	0.0131 (11)	-0.0003 (3)	0.0001 (5)	-0.0004 (5)
C4	0.4010 (5)	0.5858 (5)	0.5288 (10)	0.0047 (5)	0.0047 (5)	0.0179 (17)	-0.0004 (4)	0.0022 (7)	-0.0010 (7)
C5	0.3671 (6)	0.5735 (6)	0.3514 (10)	0.0059 (5)	0.0072 (6)	0.0157 (17)	0.0008 (4)	0.0026 (7)	0.0006 (8)
C6	0.2655 (6)	0.5476 (5)	0.3491 (9)	0.0077 (6)	0.0048 (5)	0.0098 (14)	0.0011 (4)	0.0004 (7)	-0.0010 (6)
N6	0.2797 (4)	0.4661 (4)	0.8932 (7)	0.0049 (4)	0.0042 (3)	0.0111 (10)	-0.0000 (3)	-0.0014 (5)	-0.0004 (5)
C7	0.3273 (6)	0.3923 (6)	0.9951 (9)	0.0077 (6)	0.0055 (5)	0.0121 (14)	0.0018 (5)	-0.0002 (7)	0.0010 (7)
C8	0.2605 (7)	0.3144 (5)	0.0098 (11)	0.0115 (8)	0.0034 (5)	0.0172 (18)	-0.0001 (5)	0.0000 (9)	0.0028 (7)
C9	0.1714 (6)	0.3439 (6)	0.9076 (10)	0.0082 (6)	0.0049 (5)	0.0158 (16)	-0.0013 (5)	0.0014 (8)	-0.0001 (7)

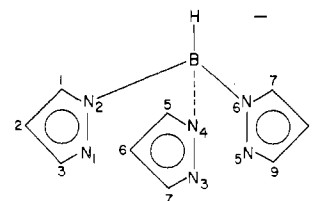
^a Estimated standard deviation in the last digit is given in parentheses. ^b β_{ij} defined by $T = \exp(\beta_{11}h^2 + \dots + 2\beta_{12}hk + \dots)$.

solutions of the complex in spectroquality dichloromethane solvent in 1-cm cells on a Cary 17 spectrophotometer. Magnetic measurements were made on a PAR vibrating magnetometer using powdered samples. A field of 5 kOe was used during the measurements. The magnetometer was calculated with the saturation moment (55.01 emu/g) of a high-purity nickel standard, and temperatures were measured with a calibrated carbon-glass resistance thermometer,⁷ the calibration of which had been checked against the paramagnetic susceptibility of chromium potassium alum. A diamagnetic correction of -276×10^{-6} emu/mol was calculated from Pascal's constants⁸ and a temperature-independent paramagnetic contribution of 120×10^{-6} emu/mol⁹ was made. A molecular weight of 624.1 was used to convert the experimental data to molar susceptibilities.

Chloro[hydrotris(1-pyrazolyl)borato]copper(II) Dimer, $\{\text{CuCl}[\text{HB}(\text{1-pz})_3]_2\}$. A solution of sodium hydrotris(1-pyrazolyl)borate (1.25 g; 5.3 mmol) in ethanol (5 mL) was added dropwise to a solution of anhydrous cupric chloride (0.7 g; 5.2 mmol) in ethanol (10 mL). The solution was allowed to stand for a few minutes at room temperature and diethyl ether (1 mL) added. After 10 min the precipitate of potassium chloride was filtered. The solution was concentrated on a rotary evaporator, without heating, when the complex precipitated as emerald green crystals. The complex was collected on a fritted glass filter and washed with diethyl ether; yield 0.88 g (53%). The complex can be crystallized by the slow addition of diethyl ether to a solution of the complex in a minimum volume of dichloromethane. Anal. Calcd for $\text{C}_9\text{H}_{10}\text{BClCuN}_6$: C, 34.6; H, 3.23; Cl, 11.4; N, 26.9. Found: C, 34.6; H, 3.32; Cl, 11.6; N, 26.7. The complex is soluble in dichloromethane and chloroform but rapidly undergoes ligand disproportionation to $\text{Cu}[\text{HB}(\text{1-pz})_3]_2$ in the presence of water. The complex undergoes an irreversible reduction at +220 mV when dissolved in dichloromethane with *tert*-butylammonium perchlorate as carrier electrolyte.

Chloro[hydrotris(1-pyrazolyl)borato]cobalt(II), $\text{CoCl}[\text{HB}(\text{1-pz})_3]$. To a stirred solution of anhydrous cobalt chloride (0.3 g; 2.3 mmol) in acetonitrile (25 mL) was slowly added a solution of sodium hydrotris(1-pyrazolyl)borate (0.5 g; 2.1 mmol) in acetonitrile (10 mL). The flask was flushed with nitrogen, and the solution was allowed to stand for 30 min. The precipitate of potassium chloride (0.11 g; 1.9 mmol) was filtered and then washed with a little acetonitrile. The combined filtrate was evaporated to dryness on a rotary evaporator. The solid was extracted with dichloromethane (~25 mL). The filtered solution was concentrated by bubbling nitrogen through the solution, and diethyl ether was added. The complex $\text{CoCl}[\text{HB}(\text{1-pz})_3]$ precipitated as a blue-green solid; yield 0.12 g (18%). The compound can be recrystallized from either dichloromethane or acetone by the slow addition of diethyl ether and then dried under vacuum at room temperature. Anal. Calcd for $\text{C}_9\text{H}_{10}\text{BClCoN}_6$: C, 35.2; H, 3.28; N, 27.3. Found: C, 35.3; H, 3.51; N, 26.2. This complex is very unstable to ligand disproportionation, and a solution of the compound in dichloromethane will precipitate anhydrous cobalt chloride if left at room temperature for more than about 30 min.

Crystal and Collection Data. Examination of the green block-shaped crystals showed them to be extensively twinned. A single crystal of

**Figure 1.** Numbering system used in the (1-pyrazolyl)borato ligand.

dimension $0.155 \times 0.155 \times 0.182$ mm was cut and mounted on a glass fiber. Preliminary X-ray analysis showed that the crystal belonged to the $P2_1/n$ space group because of systematic absences $0k0$, $k = 2n + 1$, and $h0l$, $h + l = 2n + 1$. The final lattice constants were determined from least-squares refinement of the reciprocal lattice coordinates of 12 accurately centered reflections ($\lambda_{\text{MoK}\alpha} = 0.71069$ Å) and are $a = 13.1440$ (15) Å, $b = 13.247$ (3) Å, $c = 7.467$ (13) Å, and $\beta = 96.073$ (14)°. The calculated density for two formula units per unit cell is 1.60 g/cm³.

Intensity data were collected on an automated Picker full-circle diffractometer with Zr-filtered Mo K α radiation. A total of 2249 unique reflections were collected in the range $4^\circ \leq 2\theta \leq 50^\circ$ using a θ - 2θ scan with a scan width of 2.2° with 20 steps/deg and 2s/step. The reflections $4^\circ \leq 2\theta \leq 15^\circ$ and $15^\circ \leq 2\theta \leq 50^\circ$ were collected with two separate filters of approximate transmission ratio 2.50:1. Of the 2249 reflections, 1591 were regarded as "observed", i.e., with $I \geq 3\sigma(I)$. The standard deviation of each reflection was calculated by $\sigma^2(I) = \text{TC} + \text{BG} + 0.03I^2$, where TC is total counts, BG is background counts, and $I = \text{TC} - \text{BG}$. The intensities of three reflections were monitored every 20 reflections to check for decomposition, etc. These intensities decreased by approximately 15% during data collection, and a decay correction was applied to the one quadrant of data using the DIFFRAT program before proceeding with further data treatment.

Structure Solution and Refinement. Data were corrected for absorption ($\mu = 19.3$ cm⁻¹, transmission factors ranged from 0.75 to 0.79 cm⁻¹), and the positions of the nonhydrogen atoms were obtained from MULTAN. One refinement cycle with MULTAN gave some improvement but no changes occurred with subsequent refinement. The atomic coordinates were refined further using Fourier mapping techniques. Initially only Cu and Cl were refined anisotropically, but in subsequent cycles all nonhydrogen atoms were refined in this manner. At this stage of refinement, all nonhydrogen parameters converged to an R [$= \sum ||F_o| - |F_c|| / \sum |F_o|$] of 10.6% and an R_w [$= \sum w(|F_o| - |F_c|)^2 / \sum w|F_o|^2$]^{1/2} of 7.9%, for all reflections. Difference maps at this stage revealed the coordinates of the 10 H atoms, and refinement of all parameters except hydrogen thermal parameters, which were fixed at 4.0 Å², converged to $R = 9.7\%$ and $R_w = 6.9\%$. The goodness of fit was 1.15 with $w = 1/\sigma^2(F)$.

The parameter shifts on the last cycle (some of the hydrogen positional parameters) were less than the values of their estimated errors. Scattering factor tables for Cu, Cl, N, C, B, and H were taken from ref 10. Computer programs used are part of a local library.¹¹

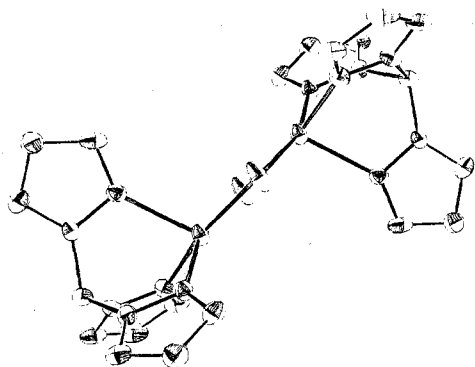


Figure 2. View of $\{\text{CuCl}[\text{HB}(1\text{-pz})_3]\}_2$.

Final parameters are listed in Table I and bond distances and angles are given in Table II. The numbering system used for the (1-pyrazolyl)borato ligand is shown in Figure 1.

Crystal and Molecular Structure

The monoclinic crystal contains two dimer molecules in the unit cell. The copper atoms are bridged by chlorides with Cu-Cl distances of 2.306 (2) and 2.316 (2) Å and a Cu-Cl-Cu angle of 94.51 (7)°. The bridge is planar, leading to a Cu-Cu separation of 3.394 (2) Å. The distances and angles in the hydrotris(1-pyrazolyl)borato ligands are similar to those reported for other such complexes, and these anions coordinate to the two coppers in an ordered manner to give a centrosymmetric dimer molecule (Figure 2). Two of the nitrogens bonded to copper (N(1) and N(5)) lie close to the plane of the Cu_2Cl_2 unit, but the third nitrogen of the tridentate ligand bonded to copper (N(3)) is out of this plane. The distances Cu-N(1) (1.992 (5) Å) and Cu-N(5) (1.985 (5) Å) are very slightly shorter than are observed for Cu-N in the copper(I) complex $\text{Cu}(\text{CO})[\text{HB}(1\text{-pz})_3]$, but the third distance Cu-N(3) (2.200 (5) Å) is very long. The geometry about each copper is best described as that of a distorted square pyramid having the ligating atoms Cl(1), Cl(2), N(1), and N(5) in the plane of the square, and the hydrotris(1-pyrazolyl)borato nitrogen, N(3), in the apical position. The distortion from this ideal geometry is essentially a small twist in the basal plane and a 17° distortion of the apical nitrogen N(3) away from the basal center.

Electronic and EPR Spectra. The electronic spectrum of the complex $\{\text{CuCl}[\text{HB}(1\text{-pz})_3]\}_2$ as a solution in dichloromethane at ambient temperature shows three broad absorptions at 8550 (24), 13 280 (120), and 36 760 (4430) cm^{-1} (extinction coefficients in parentheses). The lowest energy d-d band is at considerably lower energy than the band at 16 100 cm^{-1} in the octahedral complex $\text{Cu}[\text{HB}(1\text{-pz})_3]_2$ or the band at 18 450 cm^{-1} in the planar complex $\text{Cu}[\text{H}_2\text{B}(1\text{-pz})_2]_2$.² This direction of shift for copper(II) in a distorted square-pyramidal environment is not unexpected.¹² The position and extinction coefficient identify the low-energy band at 8550 cm^{-1} as being principally a d-d one, although the band is broad rather than split at room temperature. The complex remains a penta-coordinate dimer in dichloromethane solvent, but because of the significant distortion about the copper(II) centers, it is difficult to assign the transitions with a high degree of confidence.

The complex $\text{CoCl}[\text{HB}(1\text{-pz})_3]$ as an 8.05×10^{-3} M solution in dichloromethane shows absorptions at 6000 (19), 13 900 (158), 14 700 (200), 15 900 (shoulder), 16 950 (87), and 34 500 (1600) cm^{-1} . The low-energy line is very broad and overlaps with solvent bands. The observation of this low-energy band, along with three separated bands in the visible region of the spectrum, is manifested by other complexes having a pseudotetrahedral geometry about cobalt(II). The bands in the

Table II. Bond Distances (Å) and Angles (deg) for $\{\text{CuCl}[\text{HB}(1\text{-pz})_3]\}_2$

Distances			
Cu(1)-Cl(1)	2.306 (2)	Cu-N(3)	2.200 (5)
Cu(1)-Cl(2)	2.316 (2)	Cu-N(5)	1.985 (5)
Cu-N(1)	1.992 (5)	Cu(1)-Cu(2)	3.394 (2)
B-N(2)	1.557 (9)	B-N(6)	1.528 (9)
B-N(4)	1.541 (9)		
Ring 1			
N(1)-N(2)	1.357 (7)	C(2)-C(3)	1.389 (10)
N(2)-C(1)	1.335 (8)	C(3)-N(1)	1.319 (8)
C(1)-C(2)	1.383 (10)		
Ring 2			
N(3)-N(4)	1.372 (7)	C(5)-C(6)	1.378 (10)
N(4)-C(4)	1.351 (8)	C(6)-N(3)	1.331 (8)
C(4)-C(5)	1.363 (10)		
Ring 3			
N(5)-N(6)	1.362 (7)	C(8)-C(9)	1.384 (11)
N(6)-C(7)	1.351 (8)	C(9)-N(5)	1.339 (9)
C(7)-C(8)	1.367 (11)		
Angles			
Cl(1)-Cu(1)-Cu(2)	42.63 (5)	Cu(1)-N(1)-C(3)	136.07 (43)
Cl(2)-Cu(1)-Cu(2)	42.87 (5)	Cu(1)-Cl(1)-Cu(2)	94.51 (7)
N(1)-Cu(1)-Cl(1)	162.67 (16)	Cl(1)-Cu(1)-Cl(2)	85.49 (7)
N(1)-Cu(1)-Cl(2)	91.34 (15)	N(1)-Cu-N(3)	90.16 (19)
N(3)-Cu(1)-Cl(1)	107.15 (14)	N(1)-Cu-N(5)	88.65 (22)
N(3)-Cu(1)-Cl(2)	98.64 (14)	N(3)-Cu-N(5)	89.58 (20)
N(5)-Cu(1)-Cl(1)	92.09 (16)	Cu(1)-N(3)-N(4)	113.01 (36)
N(5)-Cu(1)-Cl(2)	171.78 (17)	Cu(1)-N(3)-C(6)	141.16 (45)
Cu(1)-N(1)-N(2)	117.41 (37)	Cu(1)-N(5)-N(6)	117.50 (39)
		Cu(1)-N(5)-C(9)	135.29 (47)
B-N(2)-N(1)	119.76 (48)	B-N(4)-C(4)	131.18 (52)
B-N(2)-C(1)	130.44 (53)	B-N(6)-N(5)	119.81 (49)
B-N(4)-N(3)	119.71 (49)	B-N(6)-C(7)	131.35 (56)
N(2)-B-N(4)	108.62 (54)	N(4)-B-N(6)	109.47 (54)
N(2)-B-N(6)	107.96 (53)		
N(1)-N(2)-C(1)	109.78 (51)	C(2)-C(3)-N(1)	111.17 (61)
N(2)-C(1)-C(2)	108.53 (62)	C(3)-N(1)-N(2)	106.50 (52)
C(1)-C(2)-C(3)	104.02 (59)		
N(3)-N(4)-C(4)	109.11 (50)	C(5)-C(6)-N(3)	111.46 (60)
N(4)-C(4)-C(5)	108.78 (63)	C(6)-N(3)-N(4)	105.69 (52)
C(4)-C(5)-C(6)	104.96 (64)		
N(5)-N(6)-C(7)	108.76 (53)	C(8)-C(9)-N(5)	110.69 (67)
N(6)-C(7)-C(8)	109.27 (68)	C(9)-N(5)-N(6)	106.56 (57)
C(7)-C(8)-C(9)	104.70 (64)		

visible region can be assigned to transitions derived from $4T_1(P) \leftarrow 4A_2(v_3)$.

The EPR spectrum of the complex $\text{CuCl}[\text{HB}(1\text{-pz})_3]$ as a powder at room temperature shows a broad isotropic line centered at $g = 2.21$ (2). The line width is 453 (26) G and no hyperfine coupling can be observed. When the sample is dissolved in dichloromethane and frozen to 77 K, two poorly resolved lines are observed at $g = 2.10$ and $g = 2.29$ and, in addition, a $\Delta M_S = 2$ transition is seen at $g = 4.19$. The latter transition is diagnostic of copper(II) dimers and is therefore in agreement with the structural data. Because of the lack of knowledge of the extent of zero-field splitting, it is not possible to readily interpret the spectrum in the $g = 2$ region. In particular, the two transitions cannot be assigned to the g_{\perp} and g_{\parallel} resonances. These lines are broad and no hyperfine coupling the ^{63}Cu and ^{65}Cu nuclei is resolved.

Magnetic Measurements. The molar susceptibilities are tabulated in Table III and the data are plotted as $\chi_m T$ vs. T in Figure 3. When plotted in this manner, nonparamagnetic susceptibilities are revealed by deviations from horizontal behavior. Such deviations are seen for the present data which only approaches a constant value of $\chi_m T$ vs. T , for $T > 200$ K. For lower temperatures the data rise indicating an increase of effective moment caused by ferromagnetic coupling within

Table III. Molar Susceptibilities^a

<i>T</i> , K	χ_m (exptl)	<i>T</i> , K	χ_m (exptl)	χ_m (theor)
1.98	0.5074	8.44	0.1299	0.1279
2.13	0.4702	9.09	0.1212	0.1199
2.18	0.4384	9.79	0.1136	0.1123
2.28	0.4450	10.53	0.1060	0.1052
2.37	0.4297	11.07	0.1011	0.1006
2.52	0.4056	11.68	0.0959	0.0958
2.56	0.4001	12.40	0.0916	0.0907
2.69	0.3826	12.57	0.0903	0.0895
2.915	0.3542	12.81	0.0885	0.0880
3.11	0.3323	13.39	0.0849	0.0844
3.26	0.3191	13.58	0.0833	0.0833
3.41	0.3060	14.69	0.0764	0.0773
3.61	0.2951	15.55	0.0723	0.0732
3.85	0.2732	17.70	0.0637	0.0645
4.24	0.2513	19.38	0.0579	0.0590
4.38	0.2436	21.41	0.0520	0.0533
4.43	0.2414	23.05	0.0482	0.0495
4.58	0.2338	24.74	0.0448	0.0460
4.68	0.2294	27.74	0.0397	0.0408
4.76	0.2239	29.87	0.0367	0.0378
5.11	0.2108	34.73	0.0317	0.0322
5.36	0.1988	38.34	0.0287	0.0289
5.42	0.1999	43.38	0.0253	0.0253
5.86	0.1835	52.17	0.0208	0.0207
6.01	0.1802	54.89	0.0197	0.0196
6.17	0.1736	60.79	0.0178	0.0176
6.40	0.1692	67.15	0.0160	0.0158
6.76	0.1605	73.95	0.0144	0.0142
7.06	0.1561	78.96	0.0134	0.0132
7.26	0.1506	86.43	0.0121	0.0120
7.60	0.1443	102.4	0.0100	0.0100
8.01	0.1372	118.9	0.0086	0.0085
8.29	0.1326	130.9	0.0078	0.0077
		166.6	0.0061	0.0060
		178.5	0.0056	0.0055
		193.5	0.0050	0.0051

^a These susceptibilities have had corrections made for diamagnetic and temperature-independent paramagnetism as described in the text. The last column lists the theoretical fit to the data based upon the two-parameter model described in the text with values of the parameters equal to $2J/k = 50.8^\circ$ and $2J'/k = -0.90^\circ$.

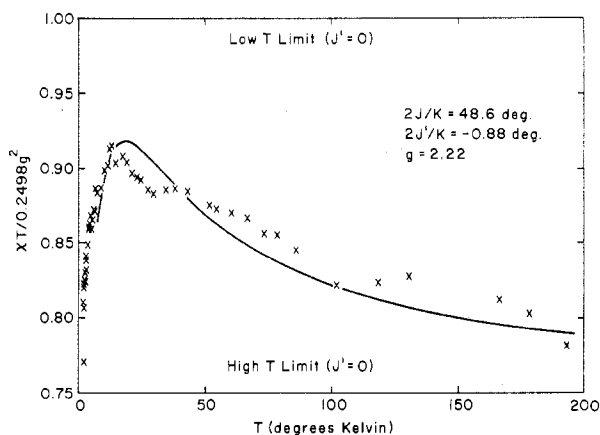


Figure 3. Normalized values of the product of χ_m vs. temperature plotted against T . The best fit curve based upon the model of Ising coupled ferromagnetic Heisenberg dimers is also shown. The upper and lower boundaries of the figure correspond to the low-temperature and high-temperature limits for a ferromagnetic dimer which is *not* coupled to neighboring dimers.

the dimer. The product reaches a maximum at about 13 K and then decreases rapidly. A plot of $1/\chi_m$ vs. T reveals Curie-Weiss behavior for $T > 70$ K with a positive temperature intercept of 10 K indicative of ferromagnetic exchange. The slope corresponds to a Curie constant per dimer of 0.935 ± 0.015 , which correlates to an EPR g value of 2.23 ± 0.02 .

The high-temperature ($T > 60$ K) data have been fit to a model which assumes the exchange Hamiltonian to be $H_{ex} = -2J\vec{S}_1 \cdot \vec{S}_2$. The susceptibility is then predicted to be

$$\chi_m = \frac{2Ng^2\mu_B^2}{3kT} \left[1 + \frac{1}{3} \exp(-2J/kT) \right]$$

where $2N\mu_B^2/3k = 0.2498$. For $g = 2.23$, the best fit is found when $2J/k = 50.8^\circ$ (35.3 cm^{-1}). J and g strongly correlate since fixing g to 2.22 gives a best fit for $2J/k = 56.2^\circ$ (39.0 cm^{-1}). This correlation causes a large imprecision on the value of $2J$ which can be deduced from the experimental data. The best value for the singlet-triplet splitting is reported as $51 \pm 10^\circ$ ($35 \pm 7 \text{ cm}^{-1}$).

A more complete model must consider the drop-off of moment which occurs below 13 K. Assuming this is due to antiferromagnetic coupling between adjacent dimers, the model of Willett et al.¹³ can be used to fit these data. This model is based upon Heisenberg coupling ($2J$) within dimers and Ising coupling ($2J'$) between dimers. Only the data above 8 K were fit to this model since the Ising interaction causes an exponential decrease of the susceptibility at low temperatures. Constraining $2J = 50.8^\circ$, $2J'/k$ is -0.90° (-0.62 cm^{-1}). Allowing both the interdimer and intradimer exchange parameters to vary simultaneously leads to the predictions of $2J/k = 48.6^\circ$ (33.7 cm^{-1}) and $2J'/k = -0.88^\circ$ (-0.61 cm^{-1}), which is an equivalent fit to the other set of parameters. A theoretical curve based on these latter parameters is plotted in Figure 3. The agreement is quite good with the systematic deviations occurring at low temperature being attributable to the nature of the Ising model. The predictions based upon this model are also tabulated in Table III for comparison with the data. The ordinate in Figure 3 has been scaled by dividing $\chi_m T$ by $0.2498g^2$, which is the Curie constant of an isolated Heisenberg dimer. Thus the ordinate value of 1.0 corresponds to the low-temperature $J' = 0$ limit. In the high-temperature limit one-quarter of the dimers will be in the nonmagnetic singlet state, so the Curie constant will drop to 0.75 of the low-temperature limit.

An alternate model¹³ assumes that the triplet ground state possesses a large zero-field splitting with the $M_S = \pm 1$ levels lying on energy D above the $M_S = 0$ level. Fitting the data to an equation for the susceptibility based upon such a model gives an equally good fit to the data as the previous model if we use $2J/k = 45^\circ$ and $D/k = 1.41^\circ$. For such a large splitting no X-band EPR spectrum would be expected and hence the model can be eliminated from consideration.

Discussion of Magnetic Data

The magnetic properties of symmetrically bridged copper-chloride dimers have recently been the object of considerable attention.¹⁴⁻¹⁸ For hydroxide-bridged dimers the singlet-triplet splitting energy has been found to vary linearly with Cu-O-Cu bridging angle, and this regularity is explained in terms of a simple molecular orbital theory.¹⁹ For the chloride-bridged copper dimers no such simple relationship has yet been found. This has been attributed in part to the fact that the singlet-triplet splittings depend on the bridging bond lengths as well as the bridging bond angle.²⁰ The bond lengths for the chlorides vary considerably (*vide infra*), whereas the oxide bridging bond lengths are uniform and do not introduce variation in J . The chloride-bridged copper dimers are also capable of assuming a number of different coordination geometries²¹⁻²⁷ which involve different orbitals in the superexchange paths. This variation, plus the limited number of examples at any specific geometry, have left the situation unclear for chloride-bridged dimers.

Structural and magnetic data are presented in Figure 4 for the known square-planar bis chloro-bridged copper dimers.

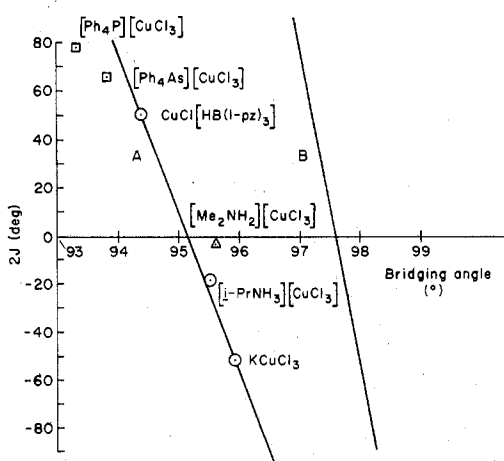


Figure 4. Heisenberg exchange parameters ($2J$) plotted against the Cu-Cl-Cu bridging angle for copper-chloride dimers. Symmetrically bridged square-planar dimers are represented by circles, unsymmetrically bridged planar dimers by triangles, and non-square-planar dimers by squares. The straight line joining the values for $\{\text{CuCl}[\text{Hb}(1\text{-pz})_3]\}_2$ and KCuCl_3 has a slope of -70 K/deg and passes through $2J = 0$ at an angle of 95.1° . The similar curve for hydroxide-bridged square-planar dimers has a slope of about -115 K/deg and passes through $2J = 0$ at 77.6° .

The first such dimer studied²¹ was KCuCl_3 which has a center of symmetry at the dimer, a bridging angle of 95° , and quite symmetric bridging Cu-Cl bond distances of 2.314 and 2.322 Å. The magnetic susceptibility was explained on the basis of an antiferromagnetic interaction with significant interdimer interaction ($J'/J = 0.05$).¹⁵ The compound $[(i\text{-PrNH}_3)\text{CuCl}_3]$ has recently been shown to also consist of a stacked chain of symmetric dimers.²⁸ The dimer has a center of symmetry, a bridging angle of 95.4° , and very similar bridging bond distances of 2.304 and 2.310 Å. The susceptibility data have been explained by the model of antiferromagnetic dimers ($2J = -19^\circ$) but with substantially greater interdimer coupling than is present in the compound KCuCl_3 . This increase in the ratio of J'/J is to be expected since the adjacent dimers are considerably nearer for $[(i\text{-PrNH}_3)\text{CuCl}_3]$ (2.698 Å) than for the KCuCl_3 compound (2.941 and 3.113 Å). The major difference between $[(i\text{-PrNH}_3)\text{CuCl}_3]$ and the previously mentioned dimers is that the $\text{Cu}_2\text{Cl}_6^{2-}$ groups deviate from square planar. This distortion arises since the planes formed by the coppers and the nonbridging chlorines are tilted with respect to the plane of the coppers and bridging chlorines.

When the exchange parameters ($2J$) for the compounds KCuCl_3 , $[(i\text{-PrNH}_3)\text{CuCl}_3]$, and $\{\text{CuCl}[\text{HB}(1\text{-pz})_3]\}_2$ are plotted against bridging angle, the three points fall very nearly in a straight line of slope approximately -70 K/deg, and which passes through $2J = 0$ at 95.1° (see Figure 4). This linearity finds a ready explanation in the molecular orbital theory proposed by Hodgson¹⁹ for the planar Cu-O-Cu dimers where the slope was found to be -115 K/deg, passing through zero exchange near 97.6° . Other salts with symmetric Cu-Cl-Cu bridges, namely, the compounds $(\text{Me}_2\text{NH}_2)\text{CuCl}_3$, $(\text{Ph}_4\text{As})\text{CuCl}_3$, and $(\text{Ph}_4\text{P})\text{CuCl}_3$, must be excluded from this

correlation either because of uncertainties in the exchange constant or because of changes in the coordination geometry. Until data are available for additional chloro-bridged dimers of copper(II), these slope and intercept values for the chloro-bridged dimers must be taken as very approximate.

Acknowledgment. This work was supported by the National Science Foundation. We thank Juanita Willett and Sue A. Roberts for assistance with the structural work and Dr. R. Gagné for useful discussions. The initial EPR work was carried out by Dr. F.-D. Tsay. D.M.R. thanks Washington State University for a leave of absence during which this project was initiated.

Registry No. $\{\text{CuCl}[\text{HB}(1\text{-pz})_3]\}_2$, 68936-68-5; $\text{CoCl}[\text{HB}(1\text{-pz})_3]$, 68936-69-6.

Supplementary Material Available: A listing of observed and calculated structure factors (11 pages). Ordering information is given on any current masthead page.

References and Notes

- (a) Washington State University. (b) California Institute of Technology.
- S. Trofimenko, *J. Am. Chem. Soc.*, **89**, 3170 (1967).
- J. P. Jesson, S. Trofimenko, and D. R. Eaton, *J. Am. Chem. Soc.*, **89**, 3148 (1967).
- C. Mealli, C. S. Arcus, J. L. Wilkinson, T. J. Marks, and J. A. Ibers, *J. Am. Chem. Soc.*, **98**, 711 (1976).
- M. R. Churchill, B. G. DeBoer, F. J. Rotella, O. M. A. Salah, and M. I. Bruce, *Inorg. Chem.*, **14**, 2051 (1975).
- J. S. Thompson, T. J. Marks, and J. A. Ibers, *Proc. Natl. Acad. Sci. U.S.A.*, **74**, 3114 (1977).
- Lake Shore Cryotronics, Columbus, Ohio 43229.
- P. W. Selwood, 2nd ed., "Magnetochemistry", Interscience, New York, 1956.
- Landolt-Börnstein, "Zahlenwerte und Function aus Physik, Chemie, Astronomie, Geophysik und Technik", New Series, Group II, Vol. 2, E. König, Ed., Springer-Verlag, Berlin, 1966.
- "International Tables for X-ray Crystallography", Vol. III, Kynoch Press, Birmingham, England, 1962, Table 3.3.1A.
- This includes modified versions of the following: Busing, Martin, and Levy's ORFLS least-squares program; Hubbard, Quicksall, and Jacobson's ALFF Fourier program; the function and error program, ORFFE, by Busing, Martin, and Levy; Johnson's ORTEP program for crystallographic illustrations; the absorption correction subroutine ORABS by Wehe, Busing, and Levy.
- (a) B. J. Hathaway, *J. Chem. Soc., Dalton Trans.*, 1196 (1972); (b) R. C. Rosenberg, C. A. Root, P. K. Bernstein, and H. B. Gray, *J. Am. Chem. Soc.*, **97**, 2092 (1975).
- C. Chow, R. D. Willett, and B. C. Gerstein, *Inorg. Chem.*, **14**, 205 (1975).
- G. J. Mauss, B. C. Gerstein, and R. D. Willett, *J. Chem. Phys.*, **46**, 401 (1967).
- K. I. Hara, M. Inoue, S. Emori, and M. Kubo, *J. Magn. Reson.*, **4**, 337 (1971).
- B. C. Gerstein, F. D. Gehring, and R. D. Willett, *J. Appl. Phys.*, **43**, 1932 (1972).
- C. Chow, R. Caputo, R. D. Willett, and B. C. Gerstein, *J. Chem. Phys.*, **61**, 271 (1974).
- M. W. Hanson, C. B. Smith, and G. O. Carlisle, *Inorg. Nucl. Chem. Lett.*, **12**, 917 (1976).
- D. J. Hodgson, *Prog. Inorg. Chem.*, **19**, 173 (1975).
- W. E. Hatfield, *A.C.S. Symp. Ser.*, No. 5, 108 (1974).
- R. D. Willett, C. Dwiggs, Jr., R. F. Kruh, and R. E. Rundle, *J. Chem. Phys.*, **38**, 2429 (1963).
- R. D. Willett, *J. Chem. Phys.*, **44**, 39 (1966).
- R. D. Willett, *J. Chem. Soc., Chem. Commun.*, 608 (1973).
- R. D. Willett and C. Chow, *Acta Crystallogr., Sect. B*, **30**, 207 (1974).
- D. W. Phelps, W. H. Goodman, and D. J. Hodgson, *Inorg. Chem.*, **15**, 2266 (1976).
- M. Textor, E. Dubler, and H. R. Oswald, *Inorg. Chem.*, **13**, 1361 (1974).
- P. G. Beckingsale, A. T. Morcom, C. E. F. Rickard, and T. N. Waters, *J. Chem. Soc., Dalton Trans.*, 2135 (1977).
- S. A. Roberts and R. D. Willett, unpublished results.